pp.141:147

ISSN: 2251-9246
EISSN: 2345-6221

Photovoltaic Microgrids Control by the Cooperative Control of Multi-Agent Systems

H.A. Shayanfar[1], S.Malek [2]

[1] Centre of Excellence for Power Automation and Operation, Electrical Engineering Department, Iran University of Science and Technology,*Tehran, Iran,Email:hashayanfar@yahoo.com,maleksajjad@yahoo.com*

Abstract

This paper presents a cooperative control which is applied to the secondary control of a microgrid controlled via a multi-agent scheme. Balancing power that leads to voltage and frequency stability in a microgrid is essential. The voltage and frequency regulations are limiting within the specified limits and conveying them to their nominal values. Limiting and conveying the voltage and frequency to their nominal values is done by the primary and secondary controls, respectively. A Microgrid has both dispatchable and non-dispatchable sources. Dispatchable sources are controlled by the conventional P-ω and Q-E droop controls. A photovoltaic as a non-dispatchable source generates the active power according to weather conditions, but the reactive power is supplied using the E-Q droop method. The E-Q droop uses the idle capacity of the inverters in the reactive power supply. Distributed secondary control increases the stability due to good, accurate and reliable controls. The frequency is constant in the whole microgrid. Since line impedances are different, load terminal voltage control is necessary. The load is considered as another agent, who can request the desired voltage at its terminal bus.

Keywords: Cooperative Control, Multi-Agent System, Secondary Control, Consensus Algorithm, Islanded Microgrid, Photovoltaic System, Frequency Control, Voltage Control

1. Introduction

Distributed Generation (DG) is integrated to the distribution grids by microgrids. A microgrid is a set of DG that is controlled as a unit and is created with the purpose of DGs management. Smart grids consist of several microgrids called microgrid clusters which communicate with a Distribution Management System (DMS).

Communication links are the smart grid essentials. A reliable and high-bandwidth communication link is usually needed, especially when the control is centralized. On the contrary, a decentralized control is preferred due to less communicated data, short distance of transmitted data and high reliability.

In view of the connection to the main grid, microgrids are categorized in two groups: 1) connected to the main grid, and 2) islanded. Microgrids, in normal operation, are connected to the main grid and exchange power with it, but when a fault occurs in the upstream grid or the power quality is very poor, the microgrid disconnects from it and is operated as an islanded microgrid. In the islanded operating mode, due to lack of a dominant source for the voltage and frequency regulations, DGs cooperate in voltage and frequency regulations. In other words, active and reactive powers sharing.

A hierarchical control scheme is used in microgrids. The hierarchical structure includes primary, secondary, and tertiary levels. The primary level uses local data and measurements. The secondary and tertiary levels need to communicate with DGs. Moreover, both the secondary and tertiary levels can be centralized or decentralized. In the islanded mode, only the primary and secondary controls are used, and they are responsible for the voltage and frequency limiting and conveying them to the nominal values, respectively.

The microgrid control by a droop control, which causes voltage and frequency deviations and decreases microgrid stability was used in [1, 2]. An angle droop method that emulates the behavior of synchronous generators was presented in [3, 4]. References [5-8]had been proposed central secondary control which needs a reliable communication and a complex structure. A centralized control development is difficult and has low reliability. A distributed secondary control for a microgrid which contains only ideal DC sources had been proposed in [9-12]. In [13],a Photovoltaic (PV) is controlled only in the grid-connected mode, but islanded operating mode is not considered.

In this paper, a PV microgrid control by the cooperative control of multi-agent systems is proposed. The cooperative control uses consensus algorithm for both voltage and frequency. The load voltage must be kept in the nominal value; therefore, the load is considered as an agent who can request the desired voltage.

2. Primary control level of microgrid

In this section, the primary level control for the dispatchable and non-dispatchable sources is addressed. The task of dispatchable sources is to regulate the voltage and frequency, and as a result, control the active and reactive powers. As the non-dispatchable sources such as a PV depend on weather conditions, they cannot control the output active power; however, the idle capacity of the inverters can be used in the reactive power supply in cooperation with the other sources by employing the $E-Q$ droop.

A. Dispatchable Sources Control

The power stage and the control scheme of the dispatchable sources are shown inFig. 1. The control is designed in the synchronous rotating frame, and *dq* transformation is used to transform the sinusoidal signals of three phases to constant signals. The control scheme includes the *P* and *Q* calculations, the droop control, and the voltage and current controllers.

The output active and reactive powers are calculated by the *P* and *Q* calculation block as follows

$$P = v_{od} i_{od} + v_{oq} i_{oq} \tag{1}$$

$$Q = -v_{od} i_{oq} + v_{oq} i_{od} \tag{2}$$

Where P and Q are the output active and reactive powers, respectively, v_{od} and v_{oq} are the components of the voltage in d and q axis, respectively, i_{od} and i_{oq} are the components of the current in *d* and *q* axis, respectively.

The well-known droop control is expressed as

$$\omega = \omega^{ref} - m_P P \tag{3}$$

$$E = E^{ref} - n_Q Q \tag{4}$$

Where ω and E are the angular frequency and voltage respectively, ω^{ref} and E^{ref} are the angular frequency and voltage set points respectively, m_P and n_Q are the droop coefficients.

The conventional proportional-integral controller is used in the voltage and current controllers. Further detailed information can be found in [14].

B. PV Control

The power stage and control system for a photovoltaic system are shown inFig. 2. It includes the *E-Q* droop control, DC link voltage, reactive power, and current controllers. A Phase Locked Loop (PLL) is used for phase angle estimation. This control system is also in the *dq* frame. The E-Q droop is proposed to use the idle capacity of PV inverters in the reactive power supply and is expressed as[8]

$$Q = \frac{E^{ref} + \delta E - E}{n_Q} \tag{5}$$

$$n_Q = \frac{\Delta E}{Q_{max}} \tag{6}$$

ΔE is the maximum allowed deviation.Q_{max} is defined as the maximum available reactive power, and is calculated as

$$Q_{max} = \sqrt{S_{rated}^2 - P_{pv}^2} \tag{7}$$

Where S_{rated} and P_{pv} are the rated PV inverter capacity and the generated active power, respectively. Block diagram of the $E-Q$ droop is illustrated inFig. 3.

3. Secondary control level

To overcome the drawbacks of the droop control, which causes voltage and frequency deviations, the secondary control is proposed in[5-7] to restore them to their nominal values as

$$\omega = \delta\omega + \omega^{ref} - m_P P \tag{8}$$

$$E = \delta E + E^{\text{ref}} - n_Q Q \tag{9}$$

Where $\delta\omega$ and δE are the signals which are generated by the secondary control.

The secondary control due to the communication with DGs can be centralized or decentralized. The centralized and decentralized secondary controls are shown in Fig. 4 and Fig. 5, respectively. In this paper, the decentralized control is applied as multi-agent systems. The consensus algorithm is used as the control protocol in this level and is introduced in the next section. Consensus Algorithm for the Secondary Control are listed in the below:

A. Vf Inverters Control

The voltage and frequency regulations are done by *Vf* controlled inverters. δE for voltage control is generated as [9]

$$e_{Ei} = e_{Load} + \sum_{j \in N_i} a_{ij}(\mathrm{v}_{\mathrm{odj}} - v_{\mathrm{odi}}) + g_i(\mathrm{E}^{\mathrm{ref}} - \mathrm{v}_{odi}) + n_{Qi}\dot{Q}_i \tag{10}$$

$$u_{Ei} = c_E e_{Ei} \tag{11}$$

$$\delta E = \int u_{Ei} dt \tag{12}$$

Where e_{Load} is the generated error from near load, N_i is the neighbors of the i the node, a_{ij} is an element of the adjacency matrix, $g_i \geq 0$ is the pinning gain and is nonzero at least for one bus and $\dot{Q}_i$ is calculated as

$$\dot{Q}_i = -\omega_c Q_i + \omega_c\left(v_{oqi} i_{odi} - v_{odi} i_{oqi}\right) \tag{13}$$

Where ω_c is the cut-off frequency of the low-pass filter (here it is considered $\omega_c = 10\pi$). $\delta\omega$ for frequency regulation is calculated as [9]

$$e_{\omega i} = \sum_{j \in N_i} a_{ij}(\omega_j - \omega_i) + g_i\left(\omega^{\text{ref}} - \omega_i\right) \tag{14}$$

$$e_{Pi} = \sum_{j \in N_i} a_{ij}(m_j P_j - m_i P_i) \tag{15}$$

$$u_{\omega i} = c_\omega e_{\omega i} \tag{16}$$

$$u_{Pi} = c_p e_{pi} \tag{17}$$

$$\delta\omega = \int \left(u_{\omega i} + u_{Pi}\right) dt \tag{18}$$

B. PQ Inverters Control

In this agent, only voltage is regulated. As a result, consensus protocol is expressed as

$$e_{Ei} = e_{Load} + \sum_{j \in N_i} a_{ij}(\mathrm{v}_{\mathrm{odj}} - v_{\mathrm{odi}}) + g_i(\mathrm{E}^{\mathrm{ref}} - \mathrm{v}_{odi}) + n_{Qi}\dot{Q}_i \tag{19}$$

$$u_{Ei} = c_E e_{Ei} \tag{20}$$

$$\delta E = \int u_{Ei} dt \tag{21}$$

C. Load Voltage Control

Critical Bus (CB) voltage regulation is important, so this agent is designed to control the voltage magnitude on its terminal. This agent's action is expressed as

$$e_{Load} = c_{Load}(E^{\text{ref}} - E_{Load}) \tag{22}$$

Where E_{Load} is the load terminal voltage.

4. Simulation Results

In order to simulate the introduced control structures, a microgrid which is shown inFig. 6, with four sources, is considered. The microgrid is simulated in MATLAB software. The microgrid has two dispatchable sources and two PV arrays. The DG-1 and DG-3 are controlled by the $P-\omega$ and $Q-E$ droop controls; DG-2 and DG-4 are controlled as the constant active power with respect to the weather conditions and $E-Q$ droop control. The consensus algorithm is used in the secondary multi-agent system. The *Vf* inverters communicate with the neighbor *Vf* inverters. Whereas the PQ inverters are connected to the close *Vf* controlled inverter. Also, loads as an agent communicate with the close agent. Microgrid data can be found in [8]. $c_P = c_\omega = c_E = 400$ and $c_{Load} = 20$ are considered as the cooperative control parameters. The *g* parameter is 1 only for DG-1 and is zero for other DGs. The adjacency matrix is defined as below. To represent the voltage regulation in the microgrid, Voltage Deviation Index (VDI) is used and calculated as [15]

$$A = \begin{bmatrix} 0 & 0 & 0 & 0 \\ 1 & 0 & 0 & 0 \\ 1 & 0 & 0 & 0 \\ 0 & 0 & 1 & 0 \end{bmatrix} \tag{23}$$

$$VDI = \sum_{i=1}^{N_{Bus}} \frac{(E_i - E_n)^2}{E_n^2} \tag{24}$$

Where E_i is the voltage at the bus i , E_n is the nominal voltage (i.e. 380V), and N_{Bus} is the number of buses.

At the start of the simulation, the PV and load agents are off. At *t*=0.5s, the *E-Q* droop of PVs is applied and PVs are attended to the reactive power sharing. It is seen that the capacity of other *Vf* inverters are released. At *t*=1s, the secondary control is performed, and the voltage and frequency approach to their nominal values; hence, the microgrid stability is improved. At *t*=1.5s, the load-1 agent is activated, and it sends the appropriate commands to DG-1

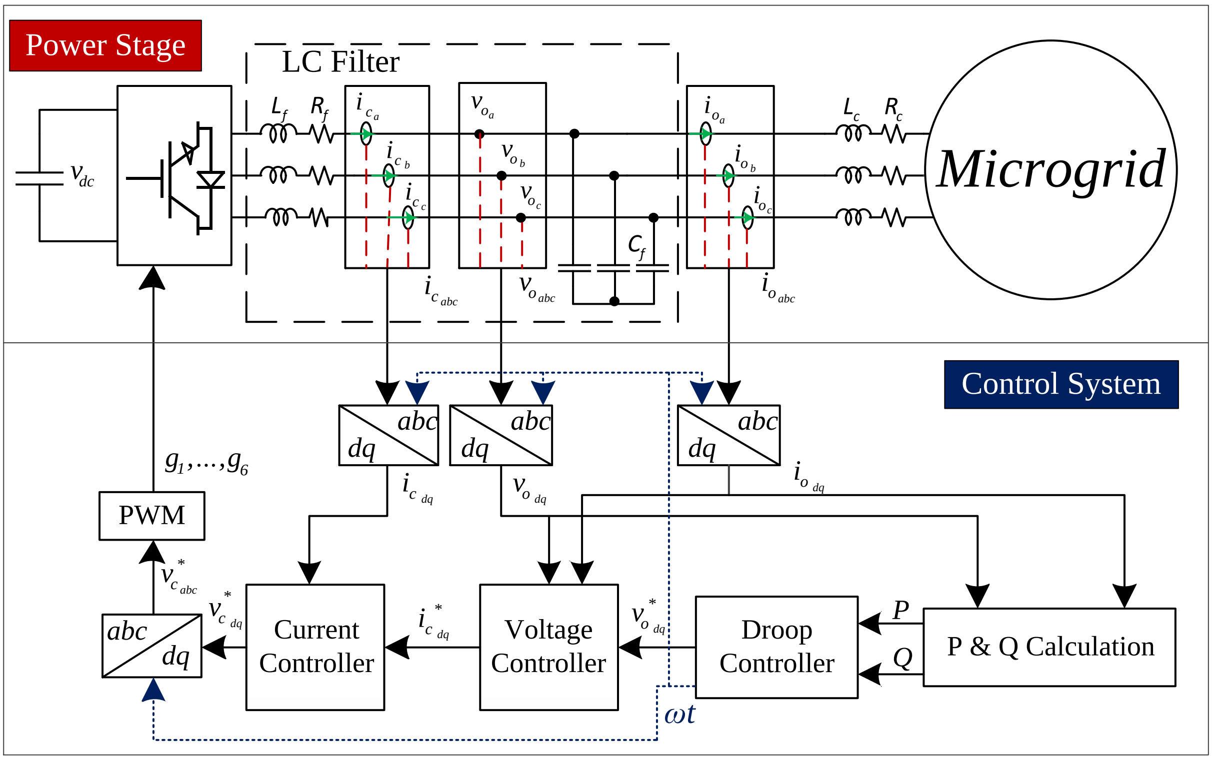

Fig. 1. Power stage and control system of the dispatchable units[8]

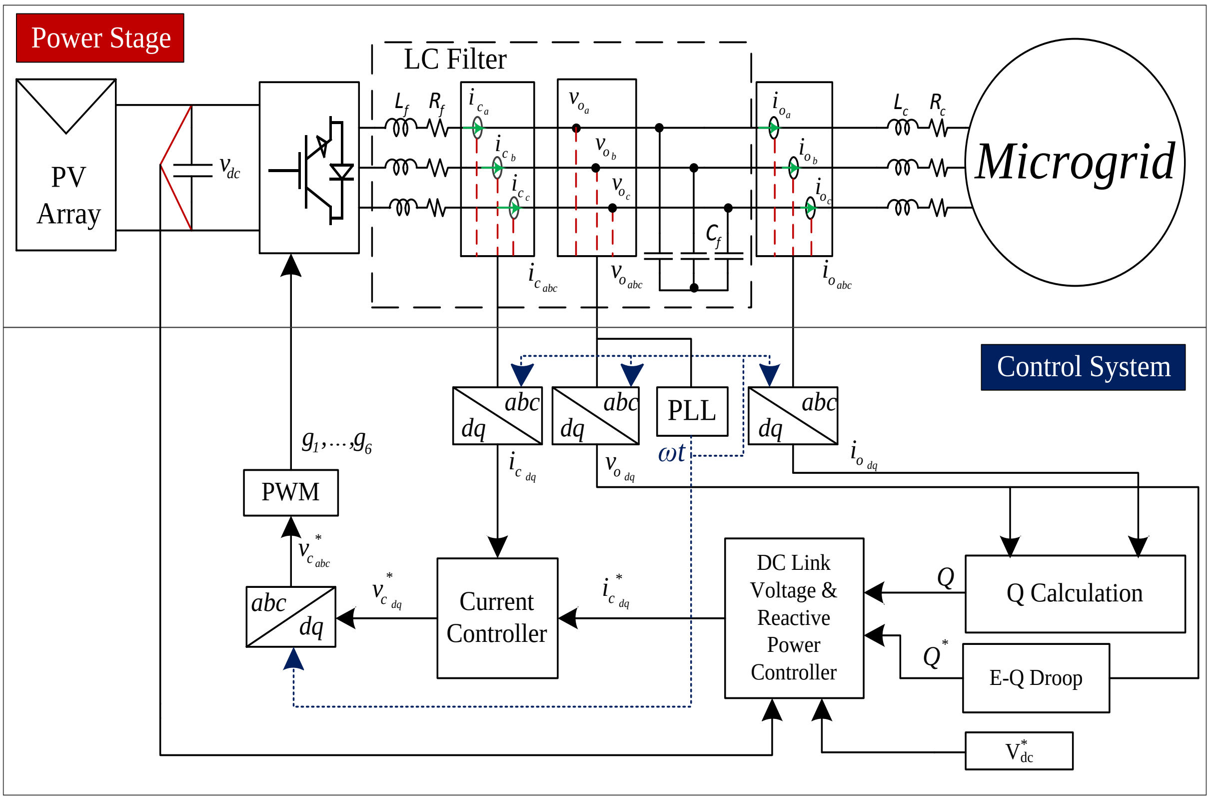

Fig. 2. Power stage and control system of the PV systems[8]

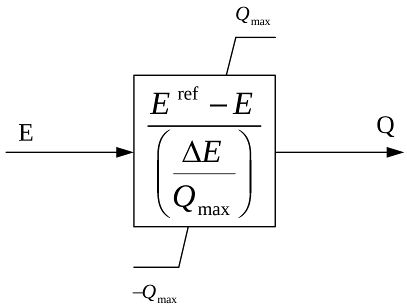

Fig. 3. $E-Q$ droop blockdiagram[8]

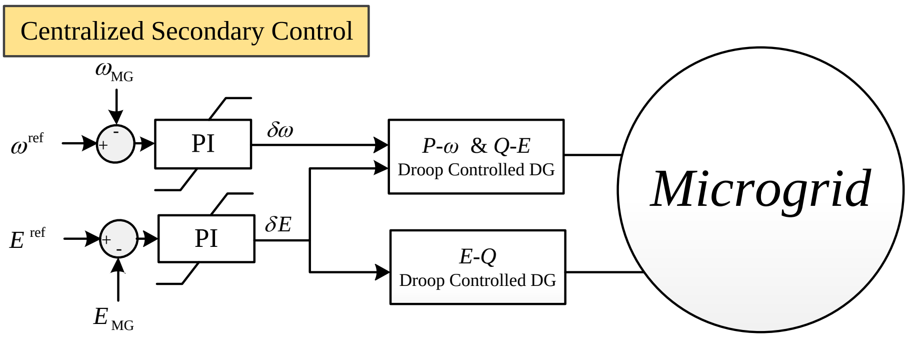

Fig. 4. Centralized microgrid secondary control in islandedmode[8]

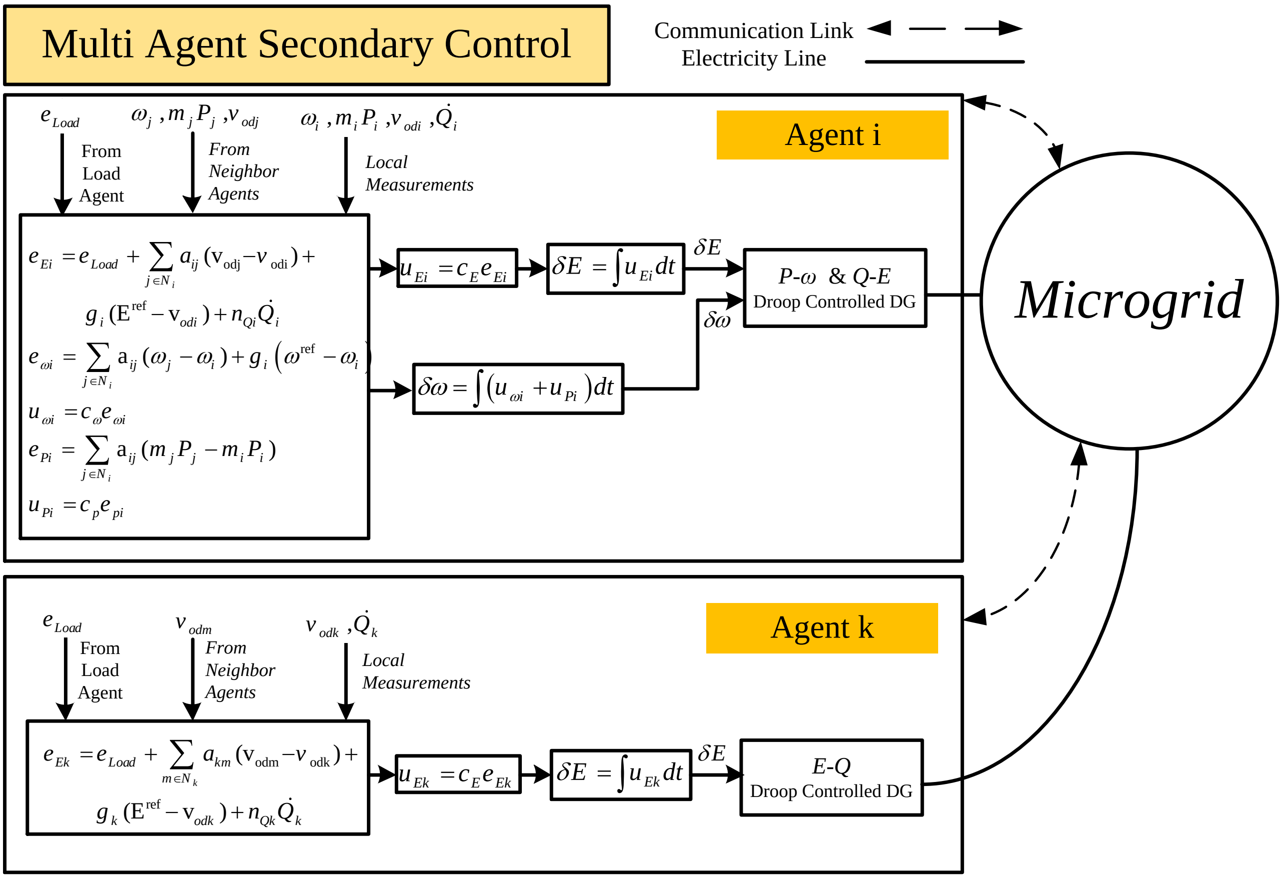

Fig. 5. Multi-agent based microgrid secondary control in islandedmode

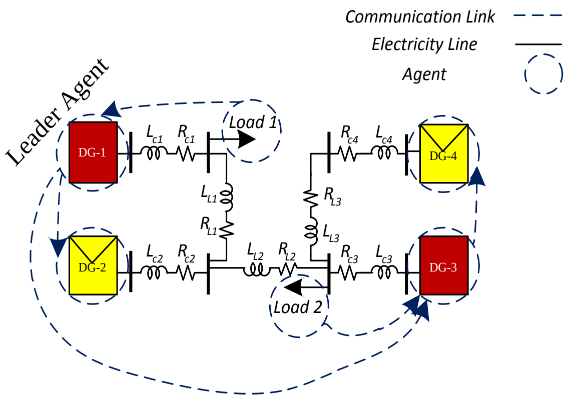

Fig. 6. Simulated microgrid structure

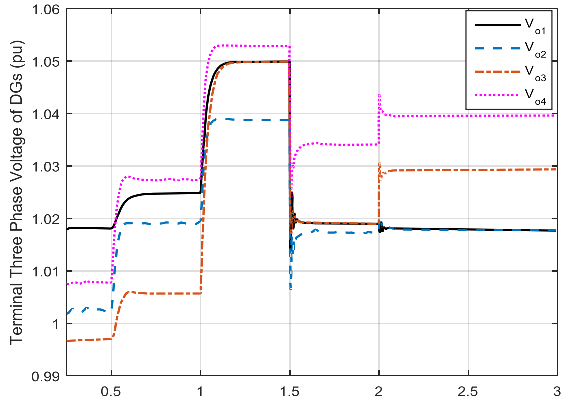

Fig. 9. Terminal three-phase voltage of DGs

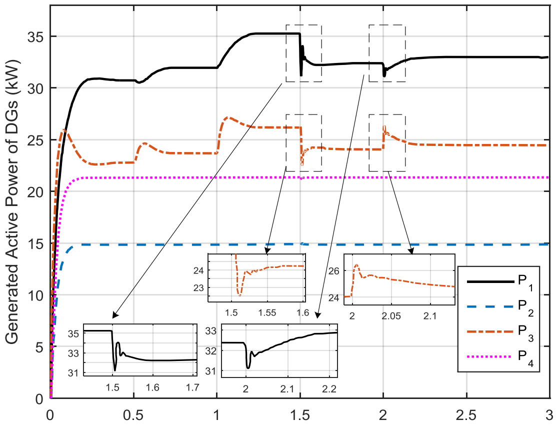

Fig. 7. Generated active power of DGs

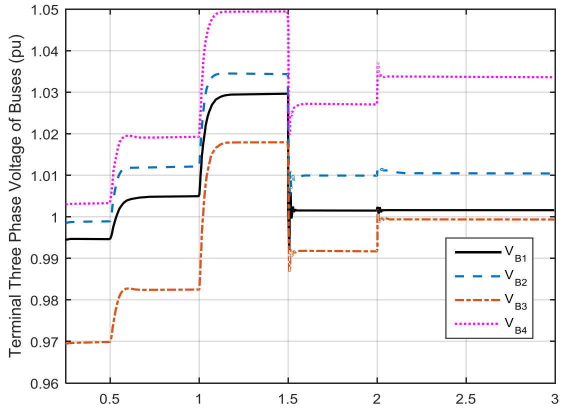

Fig. 10. Terminal three-phase voltage of buses

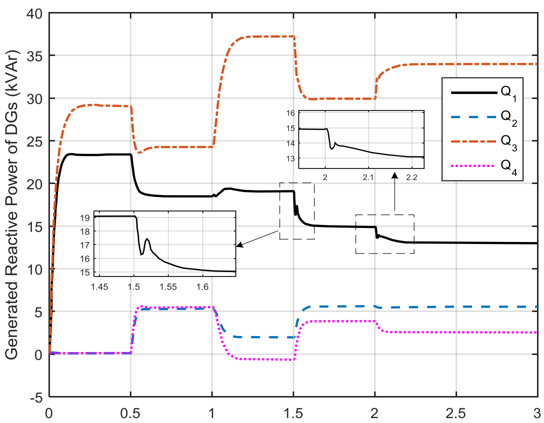

Fig. 8. Generated reactive power of DGs

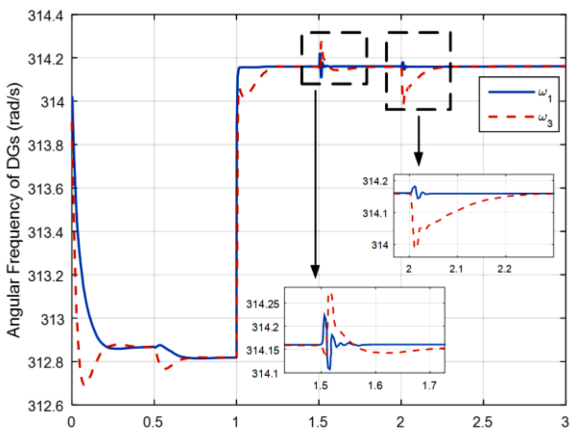

Fig. 11. Angular frequency of DGs

Table 1.
VDI in microgrid

Time Interval	V_{B1}	V_{B2}	V_{B3}	V_{B4}	VDI
0s-0.5s	378	379.6	368.7	381.3	0.000924
0.5s -1s	381.9	384.5	373.3	387.2	0.000835
1s-1.5s	391.2	393.1	386.9	398.9	0.004861
1.5s-2s	380.6	383.7	376.9	390.3	0.000899
2s-3s	380.6	384	379.8	392.7	0.001231

aiming to regulate B-1 voltage in its nominal value. At t=2s, the load-2 agent is turned on, and it regulates its terminal voltage in the nominal value. The active and reactive powers are shown inFig. 7 andFig. 8, respectively. The three-phase terminal voltage of DGs and the voltage in each bus are shown in Fig. 9 and Fig. 10, respectively. The angular frequency of DG-1 and DG-3 is shown in Fig. 11.

VDI in each time interval is given in Table I. It can be seen that the voltage regulation in specific buses has a bad effect on other buses' voltage. Load bus voltages are improved, but VDI in the microgrid deteriorates.

5. Conclusion

In this paper, a distributed secondary control based on the cooperative control of multi-agent systems for a PV Microgrid is proposed. The results show that the voltage and frequency in the microgrid approach to their nominal values. As opposed to the frequency, the voltage is not constant in the whole microgrid due to different line impedances. Hence, the load is considered as an agent who can request desired voltage magnitude. Load measures its terminal voltage and sends the error to a near agent and this agent tries to eliminate the error by adjusting the voltage reference. It can be concluded that the load voltage regulation has a bad effect on other buses. Using load as an agent, terminal voltage is regulated, but VDI in the microgrid gets worse.

References

[1] M. B. Delghavi and A. Yazdani, "Islanded-mode control of electronically coupled distributed-resource units under unbalanced and nonlinear load conditions," *Power Delivery, IEEE Transactions on,* vol. 26, pp. 661-673, 2011.

[2] J. W. Simpson-Porco, F. Dörfler, and F. Bullo, "Synchronization and power sharing for droop-controlled inverters in islanded microgrids," Automatica, vol. 49, pp. 2603-2611, 2013.

[3] M. Ashabani and Y. A.-R. Mohamed, "Integrating VSCs to weak grids by nonlinear power damping controller with self-synchronization capability," Power Systems, IEEE Transactions on, vol. 29, pp. 805-814, 2014.

[4] M. Ashabani and Y. A.-R. Mohamed, "Novel comprehensive control framework for incorporating VSCs to smart power grids using bidirectional synchronous-VSC," Power Systems, IEEE Transactions on, vol. 29, pp. 943-957, 2014.

[5] A. Bidram and A. Davoudi, "Hierarchical structure of microgrids control system," Smart Grid, IEEE Transactions on, vol. 3, pp. 1963-1976, 2012.

[6] J. M. Guerrero, J. C. Vasquez, J. Matas, D. Vicuna, L. García, and M. Castilla, "Hierarchical control of droop-controlled AC and DC microgrids—A general approach toward standardization," Industrial Electronics, IEEE Transactions on, vol. 58, pp. 158-172, 2011.

[7] J. C. Vasquez, J. M. Guerrero, J. Miret, M. Castilla, D. Vicuna, and L. García, "Hierarchical control of intelligent microgrids," Industrial Electronics Magazine, IEEE, vol. 4, pp. 23-29, 2010.

[8] H. A. Shayanfar and S. Malek, "Islanded Photovoltaic Microgrid Control With Proposed E-Q Droop and Secondary Control," presented at the International Conference and Exhibition on Solar Energy (ICESE), Tehran, 2015.

[9] A. Bidram, A. Davoudi, F. L. Lewis, and Z. Qu, "Secondary control of microgrids based on distributed cooperative control of multi-agent systems," Generation, Transmission & Distribution, IET, vol. 7, pp. 822-831, 2013.

[10] A. Bidram, A. Davoudi, F. L. Lewis, and J. M. Guerrero, "Distributed cooperative secondary control of microgrids using feedback linearization," Power Systems, IEEE Transactions on, vol. 28, pp. 3462-3470, 2013.

[11] P.-T. Cheng, C.-A. Chen, T.-L. Lee, and S.-Y. Kuo, "A cooperative imbalance compensation method for distributed-generation interface converters," Industry Applications, IEEE Transactions on, vol. 45, pp. 805-815, 2009.

[12] Q. Shafiee, J. C. Vasquez, and J. M. Guerrero, "Distributed secondary control for islanded MicroGrids-A networked control systems approach," in IECON 2012-38th Annual Conference on IEEE Industrial Electronics Society, 2012, pp. 5637-5642.

[13] A. Ghasemi, "A fuzzified multi objective Interactive S. Bae and A. Kwasinski, "Dynamic modeling and operation strategy for a microgrid with wind and photovoltaic resources," Smart Grid, IEEE Transactions on, vol. 3, pp. 1867-1876, 2012.

[14] N. Pogaku, M. Prodanović, and T. C. Green, "Modelling, analysis and testing of autonomous operation of an inverter-based microgrid," Power Electronics, IEEE Transactions on, vol. 22, pp. 613-625, 2007.

[15] F. G. Montoya, R. Baños, C. Gil, A. Espín, A. Alcayde, and J. Gómez, "Minimization of voltage deviation and power losses in power networks using Pareto optimization methods," Engineering Applications of Artificial Intelligence, vol. 23, pp. 695-703, 2010.